Water Mediated Proton Transfer in a Mesostructured Aluminosilicate Framework: An ab Initio Molecular Dynamics Study

Hong Li,*,† S. D. Mahanti,† and Thomas J. Pinnavaia‡

Department of Physics and Astronomy and Department of Chemistry, Michigan State University, East Lansing, Michigan 48824

Received: July 25, 2005; In Final Form: September 27, 2005

The proton transfer process mediated by water molecules adsorbed in an aluminosilicate framework has been studied using ab initio molecular dynamics simulations. This investigation has been carried out using a quasi-one-dimensional model simulating the mesoporous aluminosilicate channel structures. The effects of both the water loading and temperature of the system have been considered. At low coverage (one water molecule per acid site), the hydroxonium ion $(H_3O)^+$ is found to be a transition state, in agreement with earlier studies on zeolites. At a higher water coverage (two water molecules per acid site), the $(H_5O_2)^+$ species and the hydrogen bonded "neutral complex" structure are both found to be stable complexes at finite temperatures. The vibrational frequency spectrum is simulated by performing a Fourier transform of the velocity autocorrelation function (VAF), and the peak positions in the VAF are compared with IR measurements and zero-temperature calculations.

I. Introduction

Crystalline zeolites have been widely used as adsorbents, catalysts, and molecular sieves due to their uniform pore size and large internal surface area. In the past decade, mesoporous aluminosilicate (AS) materials with quasi-one-dimensional channel structures (MCM-41 and Al-MSU-S for instance) have attracted considerable attention due to their larger channel size (>1.5 nm) and their potential applications in the petroleum industry for cracking large chemical species.[1−3] By incorporating protozeolitic nanocluster precursors, also known as "zeolite seeds", into the AS framework, the hydrothermal stability of the framework is found to be greatly enhanced in comparison to its analogous derivatives assembled from conventional aluminate and silicate precursors. The hydrolytic stability of these materials in terms of energetics has been recently investigated using cluster models to simulate the mesoporous AS material incorporating five- and six-membered Si−O rings.[4] The cluster model was found to be quite reasonable.

Another area of great practical interest is the mechanism of proton transfer inside mesoporous channels in the AS framework and microporous channels in zeolites.[5−24] When water molecules are adsorbed inside the zeolite channels, proton transfer from an acidic hydroxyl group attached to the framework to water and from water back to the framework are important steps in acid catalysis by zeolites. Early IR experiments[5−8] supported the transfer of the acidic framework proton to water at low water coverage (<1 H_2O molecule per acid site) to form a stable $(H_3O)^+$ "ion-pair" structure. More recently, ^1H NMR spectroscopy[9] and IR experiments[10−13] have provided evidence favoring a "neutral complex" structure wherein water hydrogen bonds to the acidic framework proton at low water coverage. At high water coverage, proton transfer from the AS framework to water is supported by IR measurements,[11] characterized by a continuum from 3000 to 1300 cm^{-1} and two water bending modes at 1860−1650 and 1460−1450 cm^{-1}.

Extensive theoretical studies have been carried out in zeolites to address the proton transfer problem. Zero-temperature first-principles electronic structure studies for one-water-molecule adsorption[14−17] have suggested that the hydrogen bonded neutral complex structure model represents the stable adsorption structure and the ion-pair structure formed by proton transfer from the acidic site to the water is a transition state. However, ab initio molecular dynamics (MD) simulations at finite temperatures have given controversial results[18−21] for the water coverage at which proton transfer can take place. These studies suggest[18,19] that proton transfer can take place at one-water-molecule coverage for mordenite with a very short $(H_3O)^+$ lifetime of around 15 fs and for gmelinite with a much longer lifetime of around 50 fs. It also has been argued (through MD studies) that two[20] and three[21] water molecules, respectively, are needed for proton transfer to occur in HSAPO-34. The proton transfer to water controversy also has arisen for two-water-molecule coverage in ab initio ground state electronic structure calculations using cluster models. The ion-pair structure was found to be more stable than the neutral complex structure in a calculation[16] using the density functional theory (DFT) method. In a later work using the hybrid B3LYP functional,[22] just the opposite result was found; the neutral complex structure had a lower energy. Meanwhile, in another independent work of MD simulations, a $(H_5O_2)^+$ complex with a proton shared by two H_2O molecules was proposed.[23] Moreover, recent molecular dynamics simulations in gmelinite with and without extraframework Na[19,24,25] have proposed a spontaneous proton transfer process at one-water-molecule coverage.

From these reported results, it appears that proton transfer can take place under different water coverage conditions for different zeolite structures. In this work, we carry out a theoretical investigation of the proton transfer process for a mesoporous AS structure, wherein local five-membered ring subunits are present. We wanted to find out what effect the different local and global geometries (between zeolites and the mesoporous AS framework) have on the proton binding and transfer process. Since the disordered mesoporous AS framework exhibits a quasi-one-dimensional channel structure, for

* Corresponding author. E-mail: hongli@pa.msu.edu.
† Department of Physics and Astronomy.
‡ Department of Chemistry.

10.1021/jp054106y CCC: $30.25
Published on Web 11/01/2005

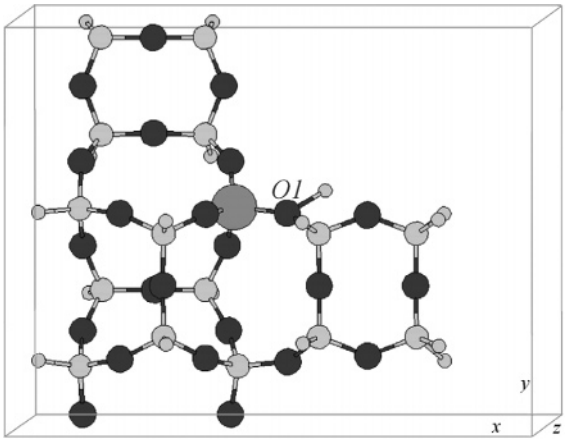

Figure 1. 1-D chain model simulating the AS framework with periodicity along the *y*-direction. The largest dark gray circle is aluminum, the other dark gray circles are oxygen, the larger light gray circles are silicon, and the smaller light gray circles are hydrogen.

our simulation studies, we have used a model AS structure containing a fragment of mesoporous framework which is repeated in one direction to simulate the one-dimensional channel geometry. Different numbers of water molecules are then incorporated into this model framework to study the dynamics of proton transfer in the presence of water molecule-(s). In the next section, we will introduce the model structure and describe the computational method. In section III, our Results and Discussion will be presented. The last section is a brief conclusion.

II. Model Structure and MD Simulations

To simulate the dynamic process of proton transfer in a mesoporous AS material, we first need to know the atomic arrangement of the AS framework. However, this information is not known, either experimentally or theoretically. In our previous ab initio calculations[4] on a mesoporous AS structure, we used cluster models to simulate the local five-membered Si−O ring structure of the AS framework, including a Brönsted acid site. We obtained results consistent with experiment findings for mesoporous AS compositions containing five-membered ring subunits.[26] In the present work, a similar model structure ($H_{17}AlSi_{15}O_{28}$) is used to simulate a part of the mesoporous AS framework incorporating five- and six-membered Si−O ring structures originally contained in BEA zeolite. However, in contrast to the cluster model in our previous work,[4] our current model structure has a one-dimensional periodicity along the *y*-direction of the unit cell, as shown in Figure 1, with the volume of the unit cell being $16.28 \times 12.66 \times 13.20$ Å^3. In this structure, the hydrogen atom bonded to O1 is the Brönsted acid proton and the other 16 hydrogen atoms are terminating atoms for the dangling bonds of silicon atoms and are not involved in the proton transfer process.

All of our calculations were performed using the Vienna ab initio simulation package (VASP)[27] with plane wave basis sets and a projector-augmented wave (PAW) method.[28] An energy cutoff of 400 eV was applied in the entire calculation and the *k*-point sampling in the total energy calculation was restricted only to the Γ point. For exchange and correlation effects, the generalized gradient approximation (GGA) of Perdew and Wang was used.[29] The total energy convergence for self-consistent iteration is 10^{-4} eV, and the force minimization for atomic geometry optimization is 0.05 eV/Å.

Ab initio molecular dynamics simulations were carried out in the microcanonical ensemble, using the Verlet velocity

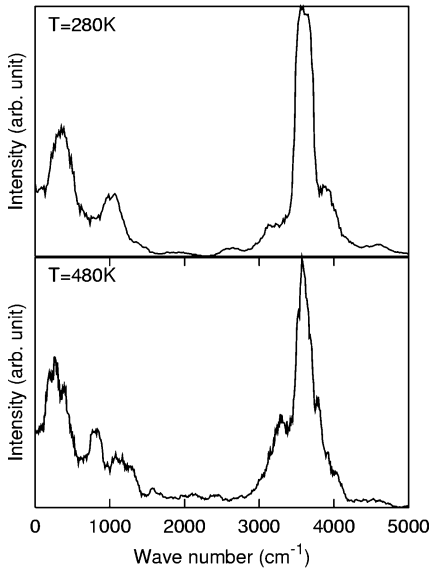

Figure 2. Frequency spectrum of the VAF projected onto the acid site proton under dehydrated conditions.

algorithm with a time step of $\Delta t = 0.5$ fs. Two different simulation temperatures (around 280 and 480 K) were chosen to simulate the water adsorption dynamics. The total simulation time at $T = 280$ K is 2 ps. The system is then heated from $T = 280$ K to $T = 480$ K within 0.8 ps by increasing the kinetic energy of the system continuously (1 K/4 fs). The simulation time around 480 K is also 2 ps.

The velocity autocorrelation function (VAF) and its Fourier transform are calculated using the application utility program P4VASP.[26] The VAF is defined as

$$C_V(t) = \frac{1}{N}\sum_{i=1}^{N}\langle \vec{V}_i(0)\cdot\vec{V}_i(t)\rangle \qquad (1)$$

where $\vec{V}_i$ is the velocity of the *i*th atom in the system and the summation is over *N*, the total number of atoms. A Fourier transform of this function reveals the underlying frequencies of the molecular dynamic processes. If we are interested in the behavior of a particular atom or a group of atoms, we can select those atoms in the summation in eq 1. The obtained frequency spectrum can be compared with the IR and inelastic neutron scattering spectrum, and the peak positions in the frequency spectrum can be compared with previous theoretical ground state calculations of vibrational frequencies.

III. Results and Discussion

A. Dynamics in the Absence of Water. The dynamics of the AS framework under dehydrated conditions was carried out around temperatures of $T = 280$ K and $T = 480$ K using the AS framework shown in Figure 1, with O1 and the attached hydrogen representing the Brönsted acid site. The Al and O1 atoms are incorporated in a five-membered ring. The O1 site is sterically more open and has been proven to have a higher protonation preference than the other neighboring oxygen atoms of Al.[4] The vibrational frequencies of the OH group in the AS structure can be studied experimentally using infrared spectroscopy, and they give information about the structure and interaction of the Brönsted acid site. The Fourier transform of the VAF projected to the hydrogen atom attached to the O1 site in Figure 1 is calculated over the duration of each MD run. The results for two different temperatures are given in Figure 2.

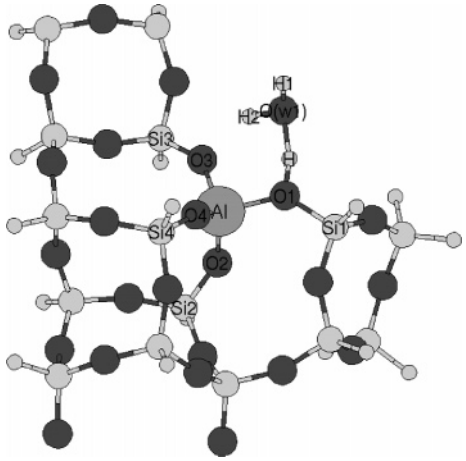

Figure 3. 1-D chain model with a water molecule adsorbed to the acid site proton. All of the labels are the same as those in Figure 1.

At lower temperature, the first peak is at about 350 cm^{-1}, which is toward the lower end of the theoretical results (421, 377, and 352 cm^{-1}) obtained from zero-temperature quantum chemical cluster calculations modeling crystalline zeolites.[16,30] This peak corresponds to the out-of-plane bending mode of the OH group (γ(OH)). The value 421 cm^{-1} obtained previously[30] is from an eight-membered ring structure, and the two lower values 377 and 352 cm^{-1} are from clusters with open structures.[16,30] Since the acid site proton in our calculation is facing toward an open space, it is understandable that our result is closer to the lower end values obtained from open structure clusters. The second peak around 1000 cm^{-1} is due to the in-plane bending of OH (δ(OH)), as described previously,[16,30] and is in excellent agreement with the values obtained from these earlier theoretical calculations (1018−1058 cm^{-1}). These two modes have been confirmed to be in the intervals 320−405 and 1052−1080 cm^{-1} by inelastic neutron scattering spectroscopy of dehydrated H-ZSM-5.[31] The high frequency peak is at about 3600 cm^{-1}. It corresponds to the OH stretching mode and is in good agreement with the experimental IR measurement[9] (3613 cm^{-1}) in H-ZSM-5 zeolites and theoretical calculations (3550−3700 cm^{-1}).[16,30] Comparing our results with other theoretical results obtained from different methods and different clusters, it is obvious that the OH vibrational frequencies are sensitive to the cluster geometry and computational method within 3%. At higher temperature, the OH stretching and out-of-plane bending mode frequencies do not show significant change from the lower temperature result.

B. Proton Transfer Dynamics in the Presence of One H_2O Molecule. For single-water-molecule coverage, we start our MD simulation at an initial geometry which is the local minimum energy state shown in Figure 3, where H represents the Brönsted acid proton. The water molecule is hydrogen bonded to the acidic proton. The covalent O1−H bond distance is 1.05 Å, whereas the hydrogen bonded O(w1)−H distance is 1.48 Å. The simulation at 280 K shows a fast proton transfer process lasting about 8 fs, which can be explained using Figure 4. When the distance between the water oxygen O(w1) and H is smaller than the distance between the framework oxygen O1 and H, the proton transfer from the acid site to H_2O takes place. However, the lifetime of the resulting $(H_3O)^+$ ion-pair structure is very short and the proton is transferred back to the framework O1 very quickly. During the subsequent MD simulation period, the proton was found to be bound to the framework O1 with the O(w1)−H distance oscillating between 1.3 and 1.9 Å.

To compare the stability of the ion-pair and neutral complex structures, we carried out ground state geometry relaxations

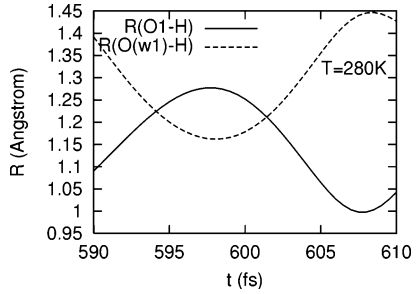

Figure 4. Time evolution of interatomic distances showing the proton transfer process with single-water-molecule coverage. The solid line is the distance between O1−H, and the dashed line is the one between O(w1)−H.

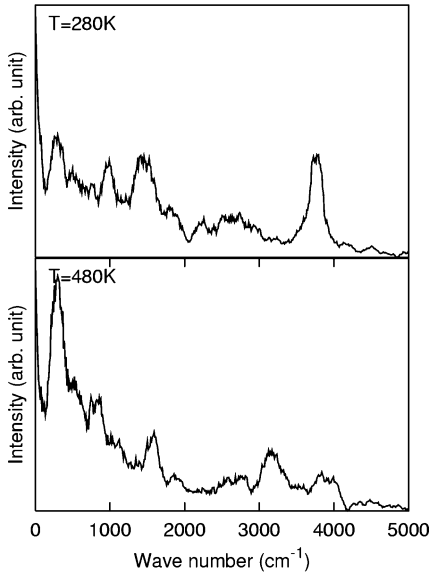

Figure 5. Frequency spectrum of the VAF projected onto the acid site proton and onto the two water hydrogen atoms for single-water-molecule coverage.

starting from several intermediate MD configurations, including ion-pair and neutral complex structures. Each geometry relaxation leads to a stable neutral complex structure, indicating that the ion-pair structure is only a transition state. At a higher temperature around 480 K, no proton transfer is observed and the water is found to be loosely bonded to proton H, with the O(w1)−H distance oscillating between 1.3 and 2.3 Å, resulting from larger thermal fluctuation of the hydrogen bond between the acid site proton and the H_2O molecule.

The Fourier transforms of VAFs projected to the three hydrogen atoms H, H1, and H2 simultaneously (see Figure 3) and to each of these three atoms separately (not shown) are calculated at two temperatures, 280 and 480 K. The results are given in Figure 5. In contrast to the dehydrated condition, central peaks are observed at both temperatures. Following the central peak, the first peak at 300 cm^{-1} is found to be associated with the collective motion of water hydrogens (H1 and H2). By projecting the VAF to the water oxygen, we confirm that this mode is a collective mode of the water molecule against the framework. A peak at 228 cm^{-1} was calculated previously and attributed to the rigid motion of the water center of mass against the framework,[30] which is in agreement with our finding. This mode shows no significant change with temperature increase. The second broad band at 550 cm^{-1} has not been reported by experiment and was not discussed in earlier studies.[16,30] A possible origin of this peak can be the water libration mode in the presence of hydrogen bonding between water and the acid

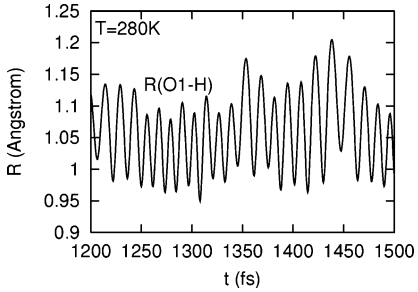

Figure 6. Time evolution of interatomic distance between O1−H with single-water-molecule coverage.

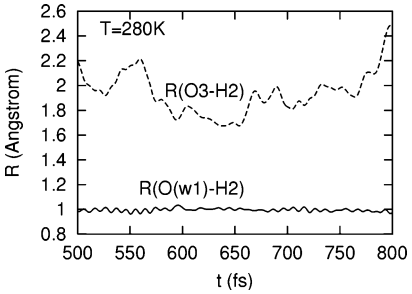

Figure 7. Time evolution of interatomic distances with single-water-molecule coverage at $T = 280$ K. The solid line is the distance between O(w1)−H2, and the dashed line is the one between O3−H2.

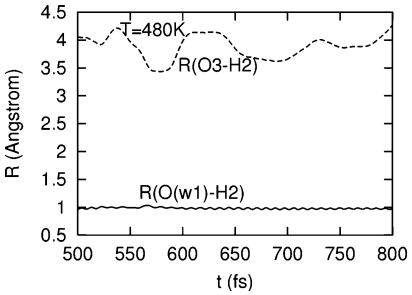

Figure 8. Time evolution of interatomic distances with single-water-molecule coverage at $T = 480$ K. The solid line is the distance between O(w1)−H2, and the dashed line is the one between O3−H2.

site proton. (For comparison, the liquid water libration frequency at $T = 273$ K is 686 cm^{-1}.) A careful ground state calculation of this mode should be carried out to check this conclusion. At lower temperature, the peak at 990 cm^{-1} corresponds to the O1−H out-of-plane bending mode (γ(OH)), which is 640 cm^{-1} larger than the result under dehydrated conditions. This difference should be attributed to the hydrogen bond between the acid site proton and the water oxygen. This peak is also observed by IR measurement[10] at 870 cm^{-1} and in neutron scattering spectra[31] at 900 cm^{-1} in H-ZSM-5. The ground state calculation results using cluster models in refs 30 and 15 fall in the interval of 844−870 and 1104 cm^{-1}. The peak at 1400 cm^{-1} is attributed to the O1−H in-plane bending mode (δ(OH)), which is 400 cm^{-1} larger than the corresponding value under dehydrated conditions. This result is in very good agreement with the IR measurement[10,11] of 1352 cm^{-1}. Thus, the two bending modes of O1−H show blue shifts due to the hydrogen bonding. The two bending mode shifts in our simulation are both larger than the values given in the ground state calculations,[30] which might be due to the thermal effect and different local geometries of the zeolite framework. At higher temperature, the out-of-plane mode shifts toward a lower frequency and the in-plane bending mode shifts toward a higher frequency compared to their lower temperature values.

The following three broad peaks at 1700, 2200−2300, and 2600−2800 cm^{-1} correspond to the *ABC* triplet[14] of O1−H stretching, which is caused by the subdivision of the very broad OH stretching band of the perturbed OH group by two Evans transmission windows at 2δ(OH) and 2γ(OH). This triplet also has been calculated,[30] and the values are 1692, 2496, and 2811 cm^{-1}, respectively. IR measurements[10,11,13] also presented values at 1700, 2400, and 2800 cm^{-1}.

An approximate O1−H stretching frequency can be calculated, as shown in Figure 6, where the O1−H distance is monitored over the whole simulation time. The result over the time interval 1200−1500 fs is given in Figure 6. An average frequency over this interval is calculated by counting the number of vibrational cycles over a given time interval, and the average value is found to be about 2500 cm^{-1}, which is 200 cm^{-1} higher than the value obtained from frequency spectrum simulation. Due to the hydrogen bonding with water, the OH stretching vibration is softened significantly from the value corresponding to the dehydrated condition of 3600 cm^{-1}.

The peak around 3100−3200 cm^{-1} corresponds to the stretching mode of the water oxygen O(w1) and hydrogen H2, which is loosely hydrogen bonded to the framework O3 at lower temperature. The approximate method used to estimate the proton O1−H stretching mode frequency (discussed above) also is applied to this mode. The O(w1)−H2 and O3−H2 distances are shown in Figures 7 and 8 for the two temperatures. The average frequencies for the two temperatures are almost the same and give a value at 3300 cm^{-1}. This value is much larger than the 3100−3200 cm^{-1} value obtained from the Fourier transform of the VAF, but it is consistent with the ground state calculations reported previously.[16] The highest frequency peak at 3700 cm^{-1} is assigned to the free O(w1)−H1 stretching mode of water. Due to the hydrogen bonding between the water hydrogen H2 and the framework oxygen O3, the stretching frequency of O(w1)−H2 is softened significantly by 500 cm^{-1} from the value of the free stretching mode.

Another interesting feature observed in our simulation is the change in hydrogen bonding between O3−H2 during the proton transfer process. Comparing Figures 4 and 7, we can see the proton transfer takes place between $t_1 = 594$ fs and $t_2 = 602$ fs. During this period, the distance between O3−H2 is at its minimum, indicating an enhanced hydrogen bonding between O3−H2. This result suggests that an increased hydrogen bonding between water hydrogen and the other framework oxygen plays an important role in the proton transfer from an acid site to the water molecule to form a $(H_3O)^+$ ion.

The simulation around $T = 280$ K for the two-water-molecule coverage starts from a local minimum energy geometry obtained by energy optimization at zero temperature, given in Figure 9, with the first-water-molecule oxygen O(w1) hydrogen bonded to the Brönsted acid proton H and the second-water-molecule oxygen O(w2) at 2.2 Å from hydrogen H2 of the first water molecule (neutral complex structure). At the beginning of the MD simulations, the second water molecule is attracted toward H2 of the first water molecule and finally forms a strong hydrogen bond (around 1.4 Å) with H2 (Figure 10). During the initial dynamic process, the acid site proton H oscillates between the framework O1 and the water oxygen O(w1). After about 0.8 ps, this proton is attracted away from the framework oxygen O1 to the water oxygen O(w1) and the $(H_5O_2)^+$ species is formed. As shown in Figure 11, the lifetime of the $(H_5O_2)^+$ species is about 0.1 ps, which is 12 times longer than the hydronium $(H_3O)^+$ lifetime seen in the single-water-molecule case. This result suggests that the $(H_5O_2)^+$ species resulting from proton transfer from the acid site in the presence of two water

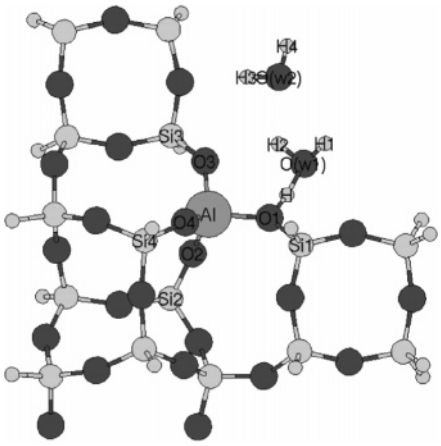

Figure 9. 1-D chain model with two water molecules adsorbed to the acid site proton, the initial geometry. All of the labels are the same as those in Figure 1.

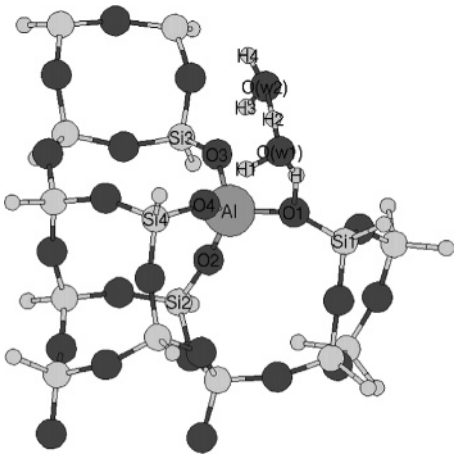

Figure 10. Snapshot of the 1-D chain model taken from a MD run in the presence of two water molecules. All of the labels are the same as those in Figure 1.

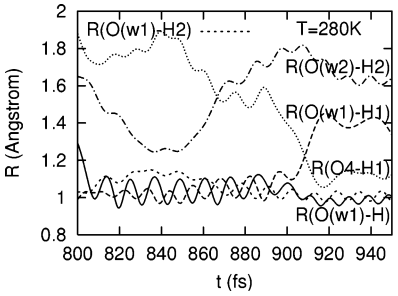

Figure 11. Time evolution of interatomic distances showing a spontaneous proton transfer process in the presence of two water molecules at $T = 280$ K.

molecules is much more stable, which is in agreement with experimental observations carried out at room temperature.[11,13]

At the end of this proton transfer process, the original acid site proton H is not transferred back to the framework oxygen O1, as in the single-water-molecule case; instead, it is strongly bonded to the water oxygen O(w1) and the original water hydrogen H1 is attracted to the framework oxygen O4 to form a new Brönsted acid site at O4. This proton transfer process can be observed in Figure 11 where the O4−H1 distance becomes smaller than 1.14 Å. As can be seen in Figure 9, the O4 site is found to be incorporated in and shared by two five-membered ring structures (Si4−O4−Al−O3−Si3 and Si4−O4−Al−O2−Si2) and exists in the same six-membered ring

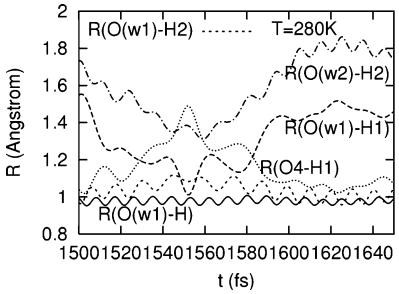

Figure 12. Time evolution of interatomic distances showing the second proton transfer process in the presence of two water molecules at $T = 280$ K.

structure (Si4−O4−Al−O1−Si1) as O1. Thus, the proton transfer process takes place from one acid site to another, both belonging to the same six-membered ring.

Following this first proton transfer process, the proton H1 oscillates between O4 and the water oxygen O(w1) and a second proton transfer process occurs during 1.53−1.58 ps (see Figure 12). In contrast to the first proton transfer, this second proton transfer process ends with H1 being attracted back to the framework O4 and the water forms a neutral complex, which is hydrogen bonded to proton H1. During these two proton transfer processes, the hydrogen bond length between H2 and O(w2) oscillates between 1.75 and 1.25 Å, most of the time being below 1.4 Å (Figures 11 and 12). This observation suggests that a strong hydrogen bond between the two water molecules in the water dimer and the dipole moment of the second water molecule are very important to the stable proton transfer process in the two-water-molecule adsorption dynamics. When the hydrogen bond length between H2 and O(w2) increases to about 1.8 Å, the H1−O4 distance decreases rapidly to less than 1.2 Å and the H1−O(w1) distance increases to about 1.4 Å. This indicates that the water hydrogen H1 is attracted to the framework oxygen O4 to form a Brönsted acid site and the $(H_5O_2)^+$ species dissociates.

We carried out geometry relaxation studies at $T = 0$, starting from several intermediate MD configurations, including ion-pair and neutral complex structures. The energy of the initial neutral complex structure adjacent to O1 (see Figure 9) is found to be about 0.3 eV higher than that of the neutral complex structure adjacent to O4, which explains the spontaneous proton transfer process from O1 to O4. The geometry relaxation results also show that the total energy of the ion-pair structure is only 0.05 eV lower than that of the neutral complex structure adjacent to the O4 site, implying that the two structures are nearly degenerate ($T = 480$ K corresponds to a thermal energy of about 0.037 eV). However, during the 2 ps dynamic simulation period at $T = 280$ K, we observed that the ion-pair structure had a total lifetime of about 150 fs in the two proton transfer processes. This might be due to the fact that the free energy of the neutral complex at finite temperature is lower than that of the ion pair, probably due to the larger entropy of the former. To further investigate this observation, a careful statistical mechanics model describing these two different structures has to constructed and studied. The energy difference of 0.05 eV between the neutral complex and the ion pair obtained here is considerably smaller than the value of 0.22 eV (21.7 kJ/mol and defined as "proton transfer energy") obtained previously.[16] Because different clusters and different basis sets were used to obtain these energies, this numerical difference can be expected. However, the large energy difference (0.22 eV) seen in ref 16 will preclude the observation of neutral complexes at T values around 300 K, in disagreement with experiment.[11,13]

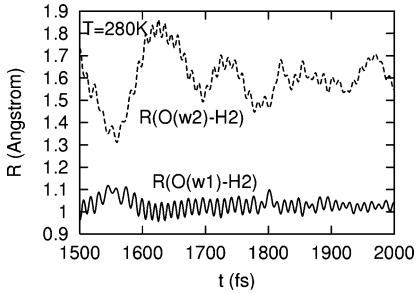

Figure 13. Time evolution of interatomic distances in the presence of two water molecules at $T = 280$ K. The solid line is the distance between O(w1)−H2, and the dashed line is the one between O(w2)−H2.

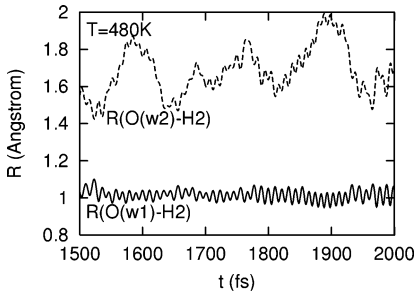

Figure 14. Time evolution of interatomic distances with single-water-molecule coverage at $T = 280$ K. The solid line is the distance between O(w1)−H2, and the dashed line is the one between O(w2)−H2.

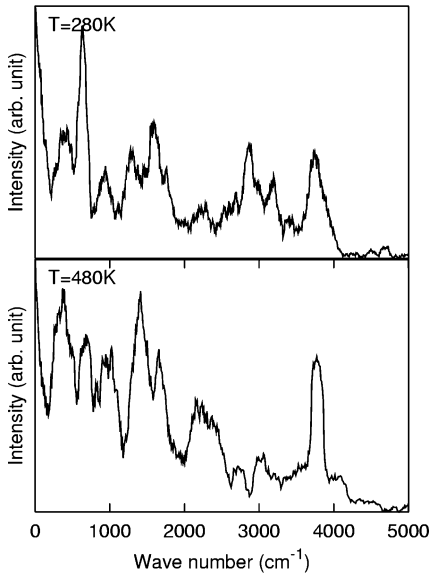

Figure 15. Frequency spectrum of the VAF projected onto the acid site proton and onto the four water hydrogen atoms in the presence of two water molecules.

At higher temperature, only very short proton transfer (from the O4 site) processes taking a few femtoseconds are observed. This can be understood from our discussion presented earlier indicating that the hydrogen bonding between the two water molecules is very important to the proton transfer process. From Figures 13 and 14, we can see that the hydrogen bonding between the two water molecules is much weaker at higher temperature, which impedes the formation of a stable $(H_5O_2)^+$ species.

Fourier transform of the VAFs projected to all five hydrogen atoms and to each of them separately also were performed at 280 and 480 K (Figure 15). The spectrum is quite complex. However, we can draw some qualitative conclusions. The spectrum at higher temperature is closer to the single-water-molecule adsorption dynamics because, at this temperature, the distance between the second-water-molecule oxygen O(w2) and the first-water-molecule hydrogen H2 is quite large (larger than 1.8 Å) and the hydrogen bonding between the two water molecules is very weak. Thus, we will focus on the lower temperature dynamics in the following discussion. Besides the central peak, the first band at 340−390 cm^{-1} corresponds to the stretching vibration of the center of mass of the water dimers. The second band at 625 cm^{-1} might be caused by the water libration hindered by the hydrogen bonding between water hydrogen and framework oxygen. The two peaks at 940 and 1270 cm^{-1} correspond to the out-of-plane and in-plane bending modes of the framework OH, as discussed for the single-water-molecule adsorption. These values are in agreement with the ground state calculation results for the neutral complex model[16] of 903 and 1257 cm^{-1}. The next major band at 1580 cm^{-1} with two shoulders is not observed in single-water-molecule dynamics and needs to be understood. From the Fourier transforms of the projections of VAFs to each hydrogen atom, this band is found to correspond to the second-water-molecule bending mode, which experiences weak hydrogen bonding between H3 and O3. In the ground state calculation of the neutral complex model,[16] the frequency of this mode is found to be at 1606 cm^{-1}. The two shoulders at 1500 and 1760 cm^{-1} are associated with the first-water-molecule bending mode, which is perturbed by hydrogen bonding between H2−O(w2) and H1−O4. The first-water-molecule bending mode has also been calculated previously for the neutral complex model[16] and is found to be 1582 cm^{-1}. The higher 1760 cm^{-1} frequency obtained in our results can be due to the bending mode of the first water molecule in short-lived $(H_5O_2)^+$ species, which is in agreement with the ground state calculation result at 1722−1744 cm^{-1} using the ion-pair model.[16] Experimental IR measurements[11] also gave peaks at 1460−1450 and 1860−1650 cm^{-1} (1621 and 1700 cm^{-1} in ref 13) as fingerprints of the presence of $(H_5O_2)^+$ species in the system. However, no experimental assignments have been made for these frequencies from the measurements.

The framework O1−H and O4−H1 stretching modes are also present in our simulations and can be compared with experiment and previous calculations. During most of the simulation time, the water dimer stays as a neutral species, with proton H attached to framework O1 at initial simulation time or H1 attached to framework O4 at a later simulation time. We first discuss the two broad bands at 2200 and 2500−2700 cm^{-1} and leave the narrow band at 2860 cm^{-1} for a separate discussion in the following paragraph. Comparing the Fourier transform analysis with the ground state calculation results for the neutral complex model,[16] the first broad band at 2200 cm^{-1} corresponds to the stretching modes of O(1)−H and O(4)−H1 when H1 is attracted to the framework oxygen O4. The O(w1)−H2 stretching mode is also strongly perturbed by the hydrogen bonding with the second water molecule, and its vibration frequency also resides in this region. The second broad band at 2500−2700 cm^{-1} corresponds to the stretching modes of O(w1)−H (after the spontaneous proton transfer process) and O(w1)−H2 during the dynamic process when the hydrogen bonds affecting these two modes are very weak.

The narrow band at 2860 cm^{-1} is found to arise from the stretching mode of O(w1)−H2 of the first water molecule, which is hydrogen bonded to the second water molecule through H2. At higher temperature, this band is shifted to 3060 cm^{-1}. To verify the projection analysis of the Fourier transform spectrum, we performed the average frequency approximation on this mode at the two temperatures. Figures 13 and 14 are used for this approximation, and the result is 2835 cm^{-1} for the lower temperature and 3035 cm^{-1} for the higher temperature; both

values are in good agreement with the Fourier transform analysis. The frequency increase at higher temperature also implies that the hydrogen bond is weaker at the higher temperature, which can be envisaged by the O(w2)−H2 distance increase shown in Figures 13 and 14.

The band at 3200 cm^{-1} is from the O(w2)−H3 stretching mode perturbed by the weak hydrogen bonding between H3 and framework oxygen O3. The highest band at about 3700 cm^{-1} is due to the stretching vibration of O(w2)−H4 and O(w1)−H when H is bonded to O(w1) and far from framework oxygen O1.

IV. Conclusions

In the present work, the proton transfer process and the vibrational dynamics associated with hydrogen motions in an AS framework containing a five-membered ring subunit are simulated (at two different temperatures) using ab initio MD calculations carried out on a model framework. The model is intended to simulate mesoporous AS materials which contain such subunits and exhibit improved acidity and hydrothermal stability in comparison to AS mesostructures lacking such subunits.[1]

With regard to the proton transfer process, we have observed a short lifetime proton transfer (∼8 fs) at a single-water-molecule coverage per acid site at 280 K. This result indicates that the ion-pair $(H_3O)^+$ structure is only a transition state, which is in agreement with recent experimental observations and zero-temperature theoretical calculations. We have also found that the strong hydrogen bonding between one of the water hydrogen atoms and the neighboring framework oxygen is the most critical factor for the proton transfer process to occur. For a two-water-molecule coverage per acid site at $T = 280$ K, the ion-pair structure has a lifetime of 100 fs, which is 12 times longer than that at single-water-molecule coverage. It is also found to have a lower total energy than a neutral complex structure. The energy difference is ∼0.05 eV, a factor of ∼4 smaller than an earlier calculation (∼0.22 eV)[16] carried out using a different method. Our results are in better agreement with IR absorption experiments[11,13] where one sees both the neutral complex and the ion pair at room temperature; an energy difference of 0.22 eV will suppress the neutral complex dramatically. We have also found that the strong hydrogen bonding between the two water molecules is essential for the proton transfer process from an acid site to the water dimer.

With regard to the vibrational dynamics, under dehydrated conditions, the OH in-plane, out-of-plane, and stretching frequencies are in excellent agreement with experimental measurements and earlier zero-temperature calculations in zeolites. For single-water-molecule coverage, blue shifts for the two bending modes of OH and the *ABC* triplet due to the OH stretching mode are obtained and are in good agreement with experimental observations and zero-temperature theoretical results. A new mode at 550 cm^{-1} is observed and is proposed to be the water libration mode. For the two-water-molecule coverage case, the OH bending modes and the water bending modes are both observed and are in agreement with the ground state calculations. The stretching mode frequencies of water and framework OH are also calculated. A blue shift of the O(w1)−H2 stretching frequency by 200 cm^{-1} at high temperature is identified from the Fourier transform of the VAF and also confirmed by average frequency estimation. This can be understood by noting that at high temperature the hydrogen bond between two H_2O molecules is much weaker than that at lower temperature.

In our future work on dynamic simulations and frequency analysis, we plan to increase the simulation time and also want to explore the anharmonic effects in OH vibrational modes. Also, because of the small mass of the proton and the low values of energy barriers, quantum tunneling effects may be important at lower temperatures. We propose to explore this issue by using the potential energy functions computed from MD simulations.

Acknowledgment. The support of this research through NSF-CRG grant CHE- 0211029 is gratefully acknowledged.

References and Notes

(1) Liu, Y.; Zhang, W.; Pinnavaia, T. J. *J. Am. Chem. Soc*. **2000**, *122*, 8791. Liu, Y.; Zhang, W.; Pinnavaia, T. J. *Angew. Chem., Int. Ed.* **2001**, *40*, 1255. Liu, Y.; Pinnavaia, T. J. *Chem. Mater.* **2002**, *14*, 3. Liu, Y.; Pinnavaia, T. J. *J. Mater. Chem*. **2002**, *12*, 3179.

(2) Zhang, Z. T.; Han, Y.; Xiao, F. S.; Qiu, S. L.; Zhu, L.; Wang, R. W.; Yu, Y.; Zhang, Z.; Zou, B. S.; Wang, Y. Q.; Sun, H. P.; Zhao, D. Y.; Wei, Y. *J. Am. Chem. Soc*. **2001**, *123*, 5014. Zhang, Z. T.; Han, Y.; Zhu, L.; Wang, R. W.; Yu, Y.; Qiu, S. L.; Zhao, D. Y.; Xiao, F. S. *Angew. Chem., Int. Ed. Engl.* **2001**, *40*, 1258. Han, Y.; Wu, S.; Sun, Y.; Li, D.; Xiao, F. S.; Liu, J.; Zhang, X.; *Chem. Mater.* **2002**, *14*, 1144.

(3) On, D. T.; Kaliaguine, S. *Angew. Chem., Int. Ed. Engl.* **2002**, *41*, 1036.

(4) Li, H.; Mahanti, S. D.; Pinnavaia, T. J. *J. Phys. Chem. B* **2005**, *109*, 2679.

(5) Ison, A.; Gorte, R. J. *J. Catal.* **1984**, *89*, 150.

(6) Jentys, A.; Warecka, G.; Derewinski, Lercher, J. A. *J. Phys. Chem.* **1989**, *93*, 4837.

(7) Aronson, M. T.; Gorte, R. J.; Farneth, W. E. *J. Catal*. **1987**, *105*, 455.

(8) Marchese, L.; Chen, J.; Wright, P.; Thomas, J. *J. Phys. Chem.* **1993**, *97*, 8109.

(9) Batamack, P.; Doremieux-Morin, C.; Fraissard, J.; Freude, D. *J. Phys. Chem.* **1991**, *95*, 3790. Batamack, P.; Doremieux-Morin, C.; Fraissard, J.; Vincent, R. *Chem. Phys. Lett.* **1991**, *180*, 545.

(10) Parker, L. M.; Bibby, D. M.; Burns, G. R. *Zeolites* **1993**, *98*, 3083.

(11) Zecchina, A.; Geobaldo, F.; Spoto, G.; Bordiga, S.; Ricchiardi, G.; Buzzoni, R.; Petrini, G. *J. Phys. Chem.* **1996**, *100*, 16584.

(12) Kondo, J. N.; Domen, K.; Hirose, C. *J. Phys. Chem*. **1996**, *100*, 1442.

(13) Kondo, J. N.; Iizuka, M.; Domen, K.; Wakabayashi, F. *Langmuir* **1997**, *13*, 747.

(14) Pelmenschikov, A. G.; van Santen, R. A. *J. Phys. Chem*. **1993**, *97*, 8109. Pelmenschikov, A. G.; van Wolput, J. H. M. C.; Hänchen, J.; van Santen, R. A. *J. Phys. Chem.* **1995**, *99*, 3612.

(15) Haase, F.; Sauer, J. *J. Phys. Chem*. **1993**, *97*, 10687.

(16) Krossner, M.; Sauer, J. *J. Phys. Chem*. **1996**, *100*, 6199.

(17) Zygmunt, S. A.; Curtiss, L. A.; Iton, L. E.; Erhardt, M. K. *J. Phys. Chem*. **1996**, *100*, 6663.

(18) Demuth, T.; Benco, L.; Hafner, J.; Toulhoat, H. *Int. J. Quantum Chem*. **2001**, *84*, 110.

(19) Jeanvione, Y.; Angyan, J. G.; Kresse, G.; Hafner, J. *J. Phys. Chem. B* **1998**, *102*, 7307.

(20) Benco, L.; Demuth, T.; Hafner, J.; Hutschka, F. *Chem. Phys. Lett*. **2000**, *324*, 373.

(21) Termath, V.; Haase, F.; Sauer, J.; Hutter, J.; Parrinello, M. *J. Am. Chem. Soc*. **1998**, *120*, 8512.

(22) Zygmunt, S. A.; Curtiss, L. A.; Iton, L. E. *J. Phys. Chem. B* **2001**, *105*, 3034.

(23) Nusterer, E.; Blöchl, P. E.; Schwarz, K. *Chem. Phys. Lett*. **1996**, *253*, 448.

(24) Benco, L.; Demuth, T.; Hafner, J.; Hutschka, F. *Microporous Mesoporous. Mater*. **2001**, *42*, 1.

(25) Benco, L.; Demuth, T.; Hafner, J.; Hutschka, F. *Chem. Phys. Lett*. **2000**, *330*, 457.

(26) Liu, Y.; Zhang, W.; Pinnavaia, T. J. *Angew. Chem., Int. Ed*. **2001**, *40*, 1255. Liu, Y.; Pinnavaia, T. J. *Chem. Mater*. **2002**, *14*, 3.

(27) Kresse, G.; Joubert, D. *Phys. Rev. B* **1999**, 59, 1758. Kresse, G.; Hafner, J. *Phys. Rev. B* **1994**, 49, 14251. Kresse, G.; Furthmüller, J. *J. Comput. Mater. Sci*. **1996**, *6*, 15.

(28) Blöchl, P. E. *Phys. Rev. B* **1994**, *50*, 17953.

(29) Perdew, J. P.; Wang, Y. *Phys. Rev. B* **1992**, *45*, 13244.

(30) Mihaleva, V. V.; van Santen, R. A.; Jansen, A. P. *J. Chem. Phys*. **2004**, *120*, 9212.

(31) Jobic, H.; Tuel, A.; Krossener, M.; Sauer, J. *J. Phys. Chem*. **1996**, *100*, 19545.